Mechanistic Diversity in the RuBisCO Superfamily: The "Enolase" in the Methionine Salvage Pathway in *Geobacillus kaustophilus*[†,‡]

Heidi J. Imker,[§] Alexander A. Fedorov,[||] Elena V. Fedorov,[||] Steven C. Almo,*[,||] and John A. Gerlt*[,§]

Departments of Biochemistry and Chemistry, University of Illinois, 600 South Mathews Avenue, Urbana, Illinois 61801, and Department of Biochemistry, Albert Einstein College of Medicine, 1300 Morris Park Avenue, Bronx, New York 10461

Received January 10, 2007; Revised Manuscript Received February 5, 2007

ABSTRACT: D-Ribulose 1,5-bisphosphate carboxylase/oxygenase (RuBisCO), the most abundant enzyme, is the paradigm member of the recently recognized mechanistically diverse RuBisCO superfamily. The RuBisCO reaction is initiated by abstraction of the proton from C3 of the D-ribulose 1,5-bisphosphate substrate by a carbamate oxygen of carboxylated Lys 201 (spinach enzyme). Heterofunctional homologues of RuBisCO found in species of *Bacilli* catalyze the tautomerization ("enolization") of 2,3-diketo-5-methylthiopentane 1-phosphate (DK-MTP 1-P) in the methionine salvage pathway in which 5-methylthio-D-ribose (MTR) derived from 5′-methylthioadenosine is converted to methionine [Ashida, H., Saito, Y., Kojima, C., Kobayashi, K., Ogasawara, N., and Yokota, A. (2003) A functional link between RuBisCO-like protein of *Bacillus* and photosynthetic RuBisCO, *Science 302,* 286−290]. The reaction catalyzed by this "enolase" is accomplished by abstraction of a proton from C1 of the DK-MTP 1-P substrate to form the tautomerized product, a conjugated enol. Because the RuBisCO- and "enolase"-catalyzed reactions differ in the regiochemistry of proton abstraction but are expected to share stabilization of an enolate anion intermediate by coordination to an active site Mg^{2+}, we sought to establish structure−function relationships for the "enolase" reaction so that the structural basis for the functional diversity could be established. We determined the stereochemical course of the reaction catalyzed by the "enolases" from *Bacillus subtilis* and *Geobacillus kaustophilus*. Using stereospecifically deuterated samples of an alternate substrate derived from D-ribose (5-OH group instead of the 5-methylthio group in MTR) as well as of the natural DK-MTP 1-P substrate, we determined that the "enolase"-catalyzed reaction involves abstraction of the 1-*proS* proton. We also determined the structure of the activated "enolase" from *G. kaustophilus* (carboxylated on Lys 173) liganded with Mg^{2+} and 2,3-diketohexane 1-phosphate, a stable alternate substrate. The stereospecificity of proton abstraction restricts the location of the general base to the N-terminal $\alpha+\beta$ domain instead of the C-terminal $(\beta/\alpha)_8$-barrel domain that contains the carboxylated Lys 173. Lys 98 in the N-terminal domain, conserved in all "enolases", is positioned to abstract the 1-*proS* proton. Consistent with this proposed function, the K98A mutant of the *G. kaustophilus* "enolase" is unable to catalyze the "enolase" reaction. Thus, we conclude that this functionally divergent member of the RuBisCO superfamily uses the same structural strategy as RuBisCO for stabilizing the enolate anion intermediate, i.e., coordination to an essential Mg^{2+}, but the proton abstraction is catalyzed by a different general base.

D-Ribulose 1,5-bisphosphate carboxylase/oxygenase (RuBisCO)[1] catalyzes the fixation of CO_2 to yield two molecules of 3-phosphoglycerate. As the major enzyme responsible for carbon assimilation, RuBisCO has attracted considerable attention because it is an inefficient catalyst: the carboxylation reaction is slow ($k_{cat} \leq 10\ s^{-1}$), and nonproductive side reactions compete with carboxylation. The latter group includes β-elimination of the C1 phosphate, isomerization

[†] This research was supported by Grant GM-65155 from the National Institutes of Health.

[‡] The X-ray coordinates and structure factors for the "enolase" complexed with inorganic phosphate, the "enolase" complexed with Mg^{2+}, the "enolase" complexed with Mg^{2+} and HCO_3^-, and the "enolase" complexed with Mg^{2+} and the stable alternate substrate DK-H 1-P have been deposited in the Protein Data Bank as entries 2OEJ, 2OEK, 2OEL, and 2OEM, respectively.

* To whom correspondence should be addressed. J.A.G.: Department of Biochemistry, University of Illinois, 600 S. Mathews Ave., Urbana, IL 61801; phone, (217) 244-7414; fax, (217) 244-6538; e-mail, j-gerlt@uiuc.edu. S.C.A.: Department of Biochemistry, Albert Einstein College of Medicine, 1300 Morris Park Ave., Bronx, NY 10461; phone, (718) 430-2746; fax, (718) 430-8565; e-mail, almo@aecom.yu.edu.

[§] University of Illinois.

[||] Albert Einstein College of Medicine.

[1] Abbreviations: "enolase", 2,3-diketo-5-methylthiopentane 1-phosphate enolase; RuBisCO, D-ribulose 1,5-bisphosphate carboxylase/oxygenase; RLP, RuBisCO-like protein; 2CABP, 2-carboxy-D-arabinitol 1,5-bisphosphate; 2C3KABP, 2-carboxyl-3-keto-D-arabinitol 1,5-bisphosphate; SeMet, selenomethionine; MTA, 5′-methylthioadenosine; MTR, 5-methylthio-D-ribose; MTR 1-P, 5-methylthio-D-ribose 1-phosphate; MTRu 1-P, 5-methylthio-D-ribulose 1-phosphate; DK-MTP 1-P, 2,3-diketo-5-methylthiopentane 1-phosphate; HK-MTP 1-P, 2-hydroxy-3-keto-5-methylthiopent-1-ene 1-phosphate; DHK-MTP, 1,2-dihydroxy-3-keto-5-methylthiopent-1-ene; KMTB, 2-keto-4-methylthiobutyrate; DK-H 1-P, 2,3-diketohexane 1-phosphate; DK-HP 1-P, 2,3-diketo-5-hydroxypentane 1-phosphate; HK-HP 1-P, 2-hydroxy-3-keto-5-hydroxypent-1-ene 1-phosphate.

10.1021/bi7000483 CCC: $37.00
Published on Web 03/13/2007

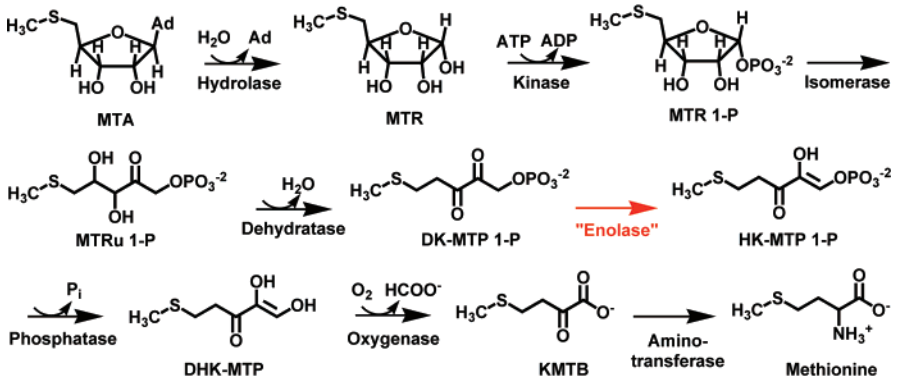

FIGURE 1: Methionine salvage pathway in species of *Bacilli* (*7*). The "enolase" in the methionine salvage pathway is the only functionally assigned member of the type IV RuBisCOs.

to D-xylulose 1,5-bisphosphate, and, most notably, oxygenation to produce 3-phosphoglycerate and 2-phosphoglycolate (*5*, *6*). The partitioning between carboxylation and the side reactions reflects alternate fates of the 1,2-*cis*-enediolate intermediate derived from abstraction of the C3 proton of the D-ribulose 1,5-bisphosphate substrate. Given this natural functional promiscuity, the recent discovery of the mechanistically diverse RuBisCO superfamily is not surprising (*7*).

Phylogenetic analyses identify four types of RuBisCOs on the basis of sequence identity and conservation of residues essential for CO_2 fixation (*7*, *8*). Type I RuBisCOs are plant, algae, and bacterial enzymes that fix CO_2 and are oligomers of four obligate dimers of large subunits and eight small subunits. Type II RuBisCOs are bacterial enzymes that fix CO_2 and are multimers of obligate dimers of divergent homologues of the type I large polypeptides. Type III RuBisCOs are archaeal enzymes that fix CO_2 and are either dimers or pentamers of obligate dimers of the large polypeptides. And, with few exceptions,[2] the type IV proteins are bacterial homologues of RuBisCO that do not fix CO_2 and are obligate dimers of homologues of the large polypeptides (*7*, *9*). Because the type IV proteins do not catalyze CO_2 fixation, these are designated "RuBisCO-like proteins" (RLPs). In all four types, the active sites are located at the interface between the smaller N-terminal $\alpha+\beta$ domain from one polypeptide and the larger C-terminal $(\beta/\alpha)_8$-barrel domain from the second polypeptide; the barrel domain contains most of the active site functional groups, including ligands for an essential Mg^{2+} and multiple acid−base catalysts.

The RuBisCO reaction mechanism involves three partial reactions: (1) general base-catalyzed enolization of the D-ribulose 1,5-bisphosphate initiated by abstraction of the C3 proton, (2) reaction of the resulting Mg^{2+}-stabilized 2,3-*cis*-enediolate intermediate with CO_2 to yield 2-carboxyl-3-keto-D-arabinitol 1,5-bisphosphate (2C3KABP), and (3) hydrolysis of 2C3KABP to yield two molecules of 3-phosphoglycerate (*5*). Structural studies reveal that the active site contains several potential acid−base catalysts, including Lys 175 (spinach enzyme numbering), His 294, and the carbamate group of carboxylated Lys 201. On the basis of the structures of liganded complexes of RuBisCO activated by carboxylation of the ϵ-amino group of Lys 201, the consensus is that the carbamate group of the carboxylated Lys 201 functions both as the general base that initiates the reaction by abstraction of the C3 proton from the D-ribulose 1,5-bisphosphate substrate and also as a ligand for an essential Mg^{2+} that stabilizes the resulting *cis*-enediolate intermediate by bidentate coordination to its O2 and O3 atoms (*5*).

Given our interests in the divergent evolution of enzyme function (*10*), we are intrigued by the RLPs. Yokota and co-workers reported that species of *Bacilli* encode a RLP that is the "enolase"[3] in the methionine salvage pathway (Figure 1) (*7*). This pathway converts 5-methylthioadenosine (MTA), a toxic byproduct of polyamine biosynthesis, to L-methionine via 5-methylthio-D-ribose (MTR). Abeles and co-workers first characterized this pathway in species of *Klebsiella*, although the pathway is now known to exist in many organisms, including *Homo sapiens* (*11*, *12*). In most organisms, a bifunctional "enolase" phosphatase that is a member of the HAD superfamily (*13*, *14*) catalyzes tautomerization of 2,3-diketo-5-methylthiopentane 1-phosphate (DK-MTP 1-P) and hydrolysis of the resulting 2-hydroxy-3-keto-5-methylthiopent-1-ene 1-phosphate (HK-MTP 1-P) to yield 1,2-dihydroxy-3-keto-5-methylthiopent-1-ene (DHK-MTP). This conjugated enol is then oxidized to formate and 2-keto-4-methylthiobutyrate (KMTB), the latter yielding methionine after transamination.

In species of *Bacilli*, the "enolase" phosphatase is replaced by two proteins, the RLP that catalyzes the "enolase" reaction and a separate member of the HAD superfamily that catalyzes the phosphatase reaction. As the only functionally assigned RLP, we were interested in establishing structure−function relationships for the "enolase" to improve our understanding of how the RuBisCO scaffold can be altered to catalyze a divergent reaction.

Although both RuBisCO and the "enolase" abstract a proton from a carbon adjacent to a carbonyl group, the regiochemistries differ (Figure 2). RuBisCO abstracts the

[2] RLPs are encoded by the genomes of the archaeon *Archaeoglobus fulgidus* (GI:11499182) and the eukaryote *Ostreococcus tauri* (GI: 116059291 and GI:116058749).

[3] Although the enzyme activity that accomplishes the keto−enol tautomerization reaction in the methionine salvage pathway has long been termed an "enolase" (*1*, *2*), the usual name for this reaction is "tautomerase". Given our interest in the members of the mechanistically diverse enolase superfamily whose members catalyze reactions that are initiated by abstraction of a proton from a carbon adjacent to a carboxylate group, including the authentic enolase in glycolysis (*3*, *4*), we would prefer not to use "enolase" to describe the keto−enol tautomerization reaction in the methionine salvage pathway. However, given the history, we compromise by using "enolase" (in quotation marks) to refer to the enzyme in the methionine salvage pathway that catalyzes the keto−enol tautomerization reaction.

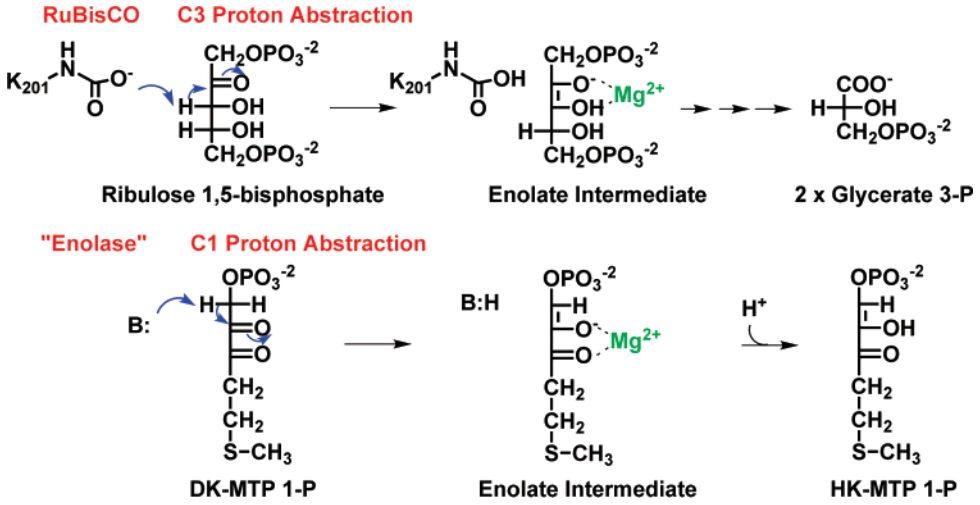

FIGURE 2: Differing regiochemistries of the enolization reactions catalyzed by the methionine salvage "enolase" and RuBisCO.

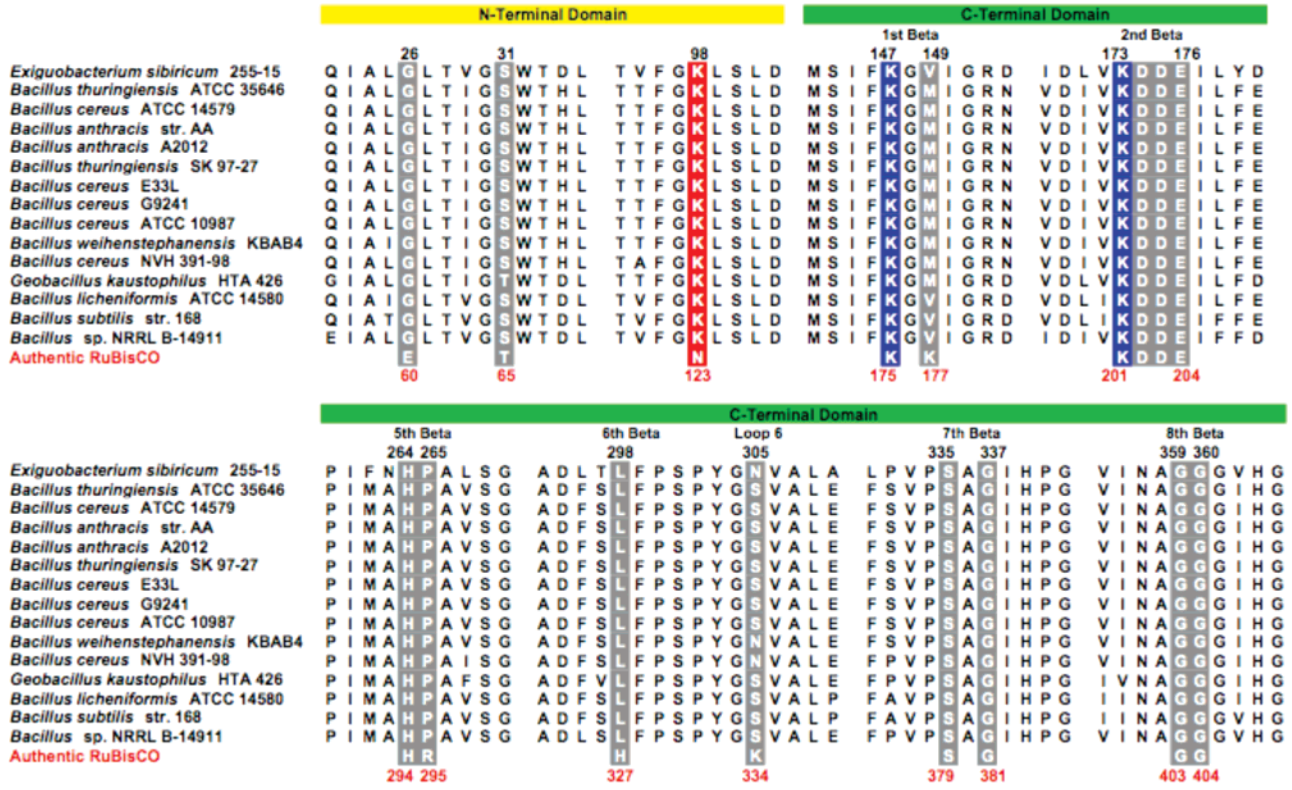

FIGURE 3: Partial sequence alignment of "enolases". Residues in the "enolases" corresponding to positions directly involved in catalysis or substrate binding in authentic RuBisCO are highlighted in gray; the sequence numbers at the top are those for the "enolase" from *G. kaustophilus*. The homologous residues in authentic RuBisCOs are shown at the bottom along with the residue numbers for spinach RuBisCO. The general base in RuBisCO is carboxylated Lys 201. As established in this article, the general base in the "enolases" is Lys 98, highlighted in red. Two other residues located in the vicinity of C1 of the substrate in the "enolases", Lys 147 and carboxylated Lys 173, are highlighted in blue.

proton from C3 of the ketose 1,5-bisphosphate substrate (D-ribulose 1,5-bisphosphate); the enolase abstracts a proton from C1 of the ketose 1-phosphate substrate (DK-MTP 1-P). This difference raises the question of whether a "new" base abstracts a proton from C1 in the "enolase" reaction.

Within the $(\beta/\alpha)_8$-barrel domain, the "enolases" share some, but not all, of the active site residues found in RuBisCOs (Figure 3). These include a KDDE motif with the carboxylated Lys (Lys 173 in the "enolases"; Lys 201 in spinach RuBisCO) as well as two carboxylate ligands for the essential Mg^{2+} that stabilizes the enediolate intermediate (Asp 175 and Glu 176 in the "enolases"; Asp 203 and Glu 204 in RuBisCO). The carbamate group of the carboxylated Lys 201 is the third ligand for the essential Mg^{2+} as well as the general base that initiates the reaction by abstraction of the proton from C3 of the D-ribulose 1,5-bisphosphate substrate. The active sites also share an additional Lys that protonates the 3-phosphoglycerate product derived from C1 and C2 of the substrate (Lys 147 in the "enolases"; Lys 175 in RuBisCO) as well as a His that catalyzes attack of water on C3 of the carboxylated intermediate to initiate cleavage of the C−C bond (His 264 in the "enolases"; His 294 in RuBisCO). Clearly, the mechanism of the RuBisCO-catalyzed reaction is much more complex than that of the

"enolase"-catalyzed reaction, so a larger number of conserved residues is expected in the RuBisCOs.

Our approach to answering this question was twofold: (1) determination of the stereochemical course of the proton abstraction catalyzed by the "enolase" so that the location of the base relative to the bound substrate could be deduced and (2) determination of the structure of the "enolase" so that appropriately located candidates for the base in the enolization reaction could be identified. We determined that the "enolases" from both *Geobacillus kaustophilus* and *Bacillus subtilis* catalyze stereospecific abstraction of the 1-*proS* proton of the DK-MTP 1-P substrate. We determined the 1.7 Å resolution structure of the activated "enolase" from *G. kaustophilus* (carboxylated on Lys 173) in the presence of 2,3-diketohexane 1-phosphate (DK-H 1-P), an alternate substrate. The alternate substrate is a bidentate ligand of the essential Mg^{2+} via its O2 and O3 atoms. Lys 98, located in the N-terminal $\alpha+\beta$ domain and conserved in all "enolases", is located on the *si* face of C1 of the ligand. On the basis of this structure, the stereochemical identity of the proton that is abstracted, and mutagenesis experiments, we conclude that Lys 98, not the carboxylated Lys 173 in the KDDE motif, is the general base in the "enolase"-catalyzed reaction. Thus, the different regiochemistry of proton abstraction in the "enolase"-catalyzed reaction is explained by a new general base. Divergent members of the RuBisCO superfamily utilize conserved elements of the RuBisCO active site to stabilize enolate anion intermediates but a general base particular to the new reaction to achieve functional diversity.

MATERIALS AND METHODS

^{1}H NMR spectra were recorded using a Varian INOVA 500NB MHz NMR spectrometer. All reagents of the highest grade commercially available were used. Deuterated D-riboses were purchased from Omicron Biochemicals (South Bend, IN). The total phosphate concentration was determined using the procedure of Ames (*15*).

Cloning, Expression, and Purification of DK-MTP 1-P "Enolase" from G. kaustophilus HTA426. The gene encoding the "enolase" (56419488) was PCR-amplified from *G. kaustophilus* HTA426 genomic DNA with primers 5′-G G A A T T C **C A T A T G** A G T G C A G T G A T G-GCAACGTATTTGC-3′ and 5′-CGC**GGATCC**TCATGCT-TCCACCTCAACGACGCCC-3′ (Bio-Synthesis, Inc.) that include a 5′-*Nde*I site and a 3′-*Bam*HI site, respectively. The PCR mixture (100 μL) contained 1 μL of 1 ng/μL template DNA, 2 μL of 50 mM $MgSO_4$, 1 μL of 2.5 units/μL platinum *Pfx* DNA polymerase (Invitrogen), 10 μL of 10× *Pfx* amplification buffer, 10 μL of 10× enhancer buffer, 2 μL of each 20 mM dNTP, 2 μL of each 20 μM forward and reverse primer, and 70 μL of ddH_2O. The PCR was performed in a PTC-200 gradient thermal cycler (MJ Research), with the following parameters: 94 °C for 3 min followed by 40 cycles of 94 °C for 1 min, 50 °C for 1.25 min, and 68 °C for 3 min; the final extension time was 10 min at 68 °C. The PCR product was purified by gel extraction (Qiagen). The amplified DNA was then restricted using *Nde*I and *Bam*HI restriction enzymes (New England Biolabs) and ligated into the pET17b expression vector (no N-terminal His tag; Novagen) using T4 DNA ligase (Fisher). The protein was expressed in *Escherichia coli* BL21(DE3) cells without induction. The bacterial culture for a typical preparation utilized 2 L of LB medium that was shaken for 36 h at 37 °C and harvested by centrifugation. The cells were resuspended in 60 mL of buffer containing 10 mM Tris-HCl (pH 7.9) containing 5 mM $MgCl_2$. The suspension was sonicated to lyse the cells. The lysate was cleared by centrifugation. The supernatant was applied to a DEAE-Sepharose FF column (2.5 cm × 50 cm, GE Healthcare) and eluted with a linear gradient (1600 mL) of 0 to 1 M NaCl buffered with 10 mM Tris-HCl (pH 7.9) containing 5 mM $MgCl_2$. Fractions containing the "enolase" were pooled and dialyzed three times against 10 mM Tris-HCl (pH 7.9) containing 5 mM $MgCl_2$ before being applied to a Q-Sepharose HP column (1.7 cm × 7 cm, GE Healthcare). The protein was eluted with a linear gradient (250 mL) of 0 to 1 M NaCl in 10 mM Tris-HCl (pH 7.9) containing 5 mM $MgCl_2$. Fractions containing >99% pure protein were pooled and dialyzed into 25 mM potassium HEPES (pH 8.0) containing 100 mM NaCl and 5 mM $MgCl_2$. The protein was concentrated to 10−25 mg/mL using a Millipore Amicon apparatus fitted with a 10 000 NMWL ultrafiltration membrane and stored at −80 °C. The protein was activated by incubation with 25 mM sodium bicarbonate at room temperature for 30−45 min before use.

Construction and Purification of Mutants. Site-directed mutants were constructed using the QuikChange method (Stratagene). The sequences of the mutants were verified by sequencing; the proteins were expressed in BL21(DE3) cells and purified as described for the wild-type "enolase".

Cloning, Expression, and Purification of Methionine Salvage Pathway Enzymes from B. subtilis Strain 168. The genes encoding the MTR kinase (GI:2633727), MTR 1-P isomerase (GI:2633726), MTRu 1-P dehydratase (GI:2633732), and the "enolase" (GI:2633730) were PCR-amplified from *B. subtilis* strain 168 genomic DNA. The genes were ligated into pET15b (Invitrogen) encoding an N-terminal six-His tag vector.

For purification, lysates were prepared from transformed *E. coli* BL21(DE3) cells as described for the "enolase". Each lysate was applied to a Ni^{2+}-charged chelating Sepharose Fast Flow column (1.5 cm × 25 cm, GE Healthcare). The column was washed with 200 mL of 20 mM Tris-HCl (pH 7.9) containing 60 mM imidazole, 0.5 M NaCl, and 5 mM $MgCl_2$, and the protein was eluted with a linear gradient (400 mL) of 60 mM to 1 M imidazole in 20 mM Tris-HCl (pH 7.9) containing 0.5 M NaCl and 5 mM $MgCl_2$. Fractions containing protein were pooled and dialyzed into 20 mM Tris-HCl (pH 7.9) containing 100 mM NaCl and 5 mM $MgCl_2$ and stored at −80 °C.

Synthesis of D-Ribose 1-Phosphate, [1-^{2}H]-D-Ribose 1-Phosphate, and [2-^{2}H]-D-Ribose 1-Phosphate. D-Ribose 1-phosphate was synthesized enzymatically using MTR kinase. A typical reaction mixture (13 mL) contained 20 mM D-ribose, 20 mM ATP, 5 mM $MgCl_2$, 5 mM DTT, and 20 mM Tris-HCl (pH 7.9). MTR kinase was added to a final concentration of 7 μM, and the reaction was allowed to proceed for <2 h; longer reaction times resulted in accumulation of a byproduct. The enzyme was removed by filtration though a 10 000 NMWL ultrafiltration membrane (Millipore), and the reaction mixture was applied to a DEAE-Sepharose FF column (1.6 cm × 7 cm) in the bicarbonate form and washed with

water. D-Ribose 1-phosphate eluted before ADP or ATP using a linear gradient (40 mL) from 0 to 0.5 M ammonium bicarbonate. Product-containing fractions were identified using a colorimetric assay for reducing sugars (*16*), pooled, and evaporated to dryness multiple times with water to remove excess ammonium bicarbonate. [1-^{2}H]-D-Ribose 1-phosphate and [2-^{2}H]-D-ribose 1-phosphate were synthesized from [1-^{2}H]- and [2-^{2}H]-D-ribose, respectively.

D-Ribose 1-phosphate: ^{1}H NMR (D_2O, 500 MHz) δ 5.48 (dd, J = 4.2, 6.4 Hz, H-1), 4.07 (q, J = 3.7, 4.2 Hz, H-4), 3.97 (ABX, J = 1.5, 4.1, 7.0 Hz, H-2), 3.93 (dd, J = 3.8, 6.3 Hz, H-3), 3.64−3.48 (ABX, J = 2.9, 4.8, 12.5 Hz, H-5).

Synthesis of D-Ribulose 1-Phosphate, [1S-^{2}H]-D-Ribulose 1-Phosphate, and [1R-^{2}H]-D-Ribulose 1-Phosphate. D-Ribulose 1-phosphate was synthesized using MTR 1-P isomerase. A typical reaction mixture (6−10 mL) contained 10 mM D-ribose 1-phosphate, 22 μM MTR 1-P isomerase, and 20 mM Tris-HCl (pH 7.5). The reaction was allowed to proceed overnight at 32 °C. The isomerase was removed by filtration through a 10 000 NMWL ultrafiltration membrane, and the reaction mixture was applied to a DEAE column in the bicarbonate form (details as described above). Product-containing fractions were evaporated to dryness; the identity of the product was confirmed by a ^{1}H NMR spectrum recorded at pD 2. [1*S*-^{2}H]-D-Ribulose 1-P and [1*R*-^{2}H]-D-ribulose 1-phosphate were synthesized from [1-^{2}H]- and [2-^{2}H]-D-ribose 1-phosphate, respectively.

D-Ribulose 1-phosphate: ^{1}H NMR (D_2O, 500 MHz) δ 4.46 (q, J = 6.0, 6.3 Hz, H-4′), 4.19 (td, J = 2.8, 5.1 Hz, H-4), 4.06−3.61 (ABX, J = 6.1, 7.0, 9.0 Hz, H-5′), 4.03 (d, J = 5.2 Hz, H-3), 3.98 (d, J = 5.9 Hz, H-3′), 3.89−3.78 (ABX, J = 2.5, 5.0, 10.1 Hz, H-5), ~3.78−3.70 (ABX, H-1′), 3.76−3.66 (ABX, J = 5.4, 5.6, 11.0 Hz, H-1).

Conversion of D-Ribulose 1-Phosphate to D-Ribulose 5-Phosphate for Determination of the Configuration of C1. [1-^{2}H]-D-Ribulose 1-phosphate was converted to [1-^{2}H]-D-ribulose in a reaction mixture (650 μL) that contained 14 mM [1-^{2}H]-D-ribulose 1-phosphate, 20 units of calf intestinal alkaline phosphatase (CIAP; Promega), 5 mM $MgCl_2$, and 15 mM potassium HEPES (pH 8.0). After 1 h at 37 °C, the reaction mixture was filtered through a 10 000 NMWL ultrafiltration membrane to remove the CIAP. To convert the [1-^{2}H]-D-ribulose to [1-^{2}H]-D-ribulose 5-phosphate, 20 mM ATP and 37 μM D-ribulokinase [RBK (*17*)] were added. The reaction was allowed to proceed for 1.5 h at 37 °C before isolation of the product by DEAE chromatography. [1-^{2}H]-D-Ribulose 5-phosphate eluted before ADP and ATP using a linear gradient from 0 to 0.5 M triethylammonium bicarbonate (pH 7.5) as described above. Product-containing fractions were evaporated to dryness and resuspended in 800 μL of D_2O, and the ^{1}H NMR spectrum was recorded.

Conversion of D-Ribulose 1-Phosphate to HK-HP 1-P. D-Ribulose 1-phosphate was converted to 2-hydroxy-3-keto-5-hydroxypent-1-ene 1-phosphate (HK-HP 1-P) by the "enolase" in the presence of limiting MTRu 1-P dehydratase. The dehydratase and "enolase" were exchanged into D_2O containing 5 mM $MgCl_2$, 100 mM NaCl, and 20 mM potassium phosphate buffer (pD 7.6) by a minimum of three successive concentrations and dilutions using a 3 mL Amicon apparatus with a 10 000 NMWL ultrafiltration membrane. The reaction mixture (800 μL) contained 5 mM D-ribulose 1-phosphate, 5 mM $MgCl_2$, 15 mM $NaHCO_3$, 1 mM maleate (as an integration standard), and 20 mM potassium phosphate (pD 7.6). The "enolase" from either *B. subtilis* or *G. kaustophilus* was added to a final concentration of 200 or 60 μM, respectively, and the reaction was initiated by addition of 15 μM MTRu 1-P dehydratase. The appearance of the HK-HP 1-P product was monitored by recording ^{1}H NMR spectra as a function of time. Reactions with the deuterated substrates were performed under the same conditions except that the substrate concentration was 3 mM.

HK-HP 1-P: ^{1}H NMR (D_2O, 500 MHz) δ 7.34 (d, J = 8.2 Hz, H-1), 3.73 (d, J = 5.8 Hz, H-5), 2.68 [t (broad), J = 5.6 Hz, H-4].

Synthesis of MTR, [1-^{2}H]MTR, and [2-^{2}H]MTR. The 2,3-*O*-isopropylidene derivative of methyl D-ribofuranoside (*18*) was converted to MTR following the procedure described by Meyers and Abeles (*19*). [1-^{2}H]MTR and [2-^{2}H]MTR were synthesized from [1-^{2}H]- and [2-^{2}H]-D-ribose, respectively.

Synthesis of MTR 1-P, [1-^{2}H]MTR 1-P, and [2-^{2}H]MTR 1-P. MTR 1-P was synthesized from MTR using MTR kinase. A typical reaction mixture (10 mL) contained 15 mM MTR, 20 mM ATP, 5 mM $MgCl_2$, 5 mM DTT, and 20 mM Tris-HCl (pH 7.9). MTR kinase was added to a final concentration of 13 μM, and the reaction was allowed to proceed for 12 h at 37 °C. The enzyme was removed by filtration though a 10 000 NMWL ultrafiltration membrane, and the reaction mixture was applied to a DEAE-Sepharose FF column (1 cm × 7 cm, bicarbonate form) and washed with water. MTR 1-P eluted before ADP or ATP using a linear gradient (40 mL) from 0 to 0.5 M ammonium bicarbonate. Product-containing fractions were evaporated to dryness multiple times from water to remove excess ammonium bicarbonate. [1-^{2}H]MTR 1-P and [2-^{2}H]MTR 1-P were synthesized from [1-^{2}H]- and [2-^{2}H]MTR, respectively.

MTR 1-P: ^{1}H NMR (D_2O, 500 MHz) δ 5.49 (dd, J = 4.3, 6.3 Hz, H-1), 4.21 (td, J = 3.9, 5.9 Hz, H-4), 4.06 (ABX, J = 1.7, 4.1, 6.5 Hz, H-2), 3.91 (dd, J = 3.7, 6.4 Hz, H-3), 2.71−2.58 (ABX, J = 5.6, 6.3, 13.9 Hz, H-5), 2.04 (s, H-6).

Synthesis of MTRu 1-P, [1S-^{2}H]MTRu 1-P, and [1R-^{2}H]-MTRu 1-P. MTRu 1-P was synthesized using MTR 1-P isomerase. A typical reaction mixture (800 μL) contained 5 mM MTR 1-P, 20 μM MTR 1-P isomerase, and 20 mM phosphate buffer (pD 7.5). The reaction mixture was incubated at room temperature for 1 h, and the product was used without isolation. [1*S*-^{2}H]MTRu 1-P and [1*R*-^{2}H]MTRu 1-P were synthesized from [1-^{2}H]MTR 1-P and [2-^{2}H]MTR 1-P, respectively.

MTRu 1-P: ^{1}H NMR (D_2O, 500 MHz) δ 4.55−4.43 (ABX, J = 6.4, 19.0 Hz, H-1), 4.25 (d, J = 5.0 Hz, H-3), 3.90 (dt, J = 4.9, 8.1 Hz, H-4), 2.57−2.42 (ABX, J = 4.7, 8.3, 14.0 Hz, H-5), 1.89 (s, H-6).

Conversion of MTRu 1-P to HK-MTP 1-P. MTRu 1-P was converted to HK-MTP 1-P by the "enolase" in the presence of a limiting amount of MTRu 1-P dehydratase. Reaction mixtures (800 μL) contained 5 mM MTRu 1-P, 5 mM $MgCl_2$, 15 mM $NaHCO_3$, 1 mM maleate, and 20 mM phosphate buffer (pD 7.6). The DK-MTP 1-P "enolase" from *B. subtilis* or *G. kaustophilus* was added to a final concentration of 10 μM, and the reaction was initiated by addition of 1 μM MTRu 1-P dehydratase. The appearance of the HK-MTP 1-P product was monitored by recording ^{1}H NMR spectra as a function of time.

Table 1: Data Collection and Refinement Statistics

	SeMet·E·PO_4	E·Mg	E·Mg·HCO_3	E·Mg·DK-H 1-P
		Data Collection		
beamline	NSLS X9A	NSLS X4A	NSLS X4A	NSLS X4A
wavelength (Å)	0.97811 (peak)	0.979	0.979	0.979
space group	$P3_221$	$C2$	$C2$	$C2$
no. of molecules in arbitrary unit	2	2	2	2
unit cell parameters				
a (Å)	132.67	130.76	130.70	130.35
b (Å)		59.54	59.01	59.80
c (Å)	167.47	109.28	109.47	109.35
β (deg)		103.24	103.28	103.54
resolution (Å)	2.55	1.8	1.8	1.7
no. of unique reflections	54519	74695	73839	86288
completeness (%)	97.6	98.3	97.	95.7
R_{merge}	0.068	0.044	0.045	0.059
average I/σ	38.3	29.6	29.2	24.1
		Refinement		
resolution (Å)	25.0−2.55	25.0−1.8	25.0−1.8	25.0−1.7
R_{cryst}	0.237	0.184	0.196	0.191
R_{free}	0.245	0.207	0.220	0.209
rmsd for bonds (Å)	0.007	0.006	0.007	0.006
rmsd for angles (deg)	1.5	1.3	1.4	1.4
no. of protein atoms	6273	6338	6338	6308
no. of waters	73	727	668	603
no. of Mg^{2+} ions	0	2	2	2
Lys 173 carboxyl	no	yes	yes	yes
bound ligand	PO_4	Mg^{2+}	Mg^{2+}, HCO_3	Mg^{2+}, DK-H 1-P
ligand atoms	10		8	19
PDB entry	2OEJ	2OEK	2OEL	2OEM

HK-MTP 1-P: ^{1}H NMR (D_2O, 500 MHz) δ 7.38 (d, J = 8.2 Hz, H-1), 2.80 [t (broad), J = 7.0 Hz, H-4], 3.73 (d, J = 7.0 Hz, H-5), 1.89 (s, H-6).

Spectrophotometric Assay Using 2,3-Diketohexane 1-Phosphate. 2,3-Diketohexane 1-phosphate (DK-H 1-P), a desthio alternate substrate previously reported to be a substrate for the "enolase" phosphatase from *Klebsiella*, was synthesized according to the literature procedure (*20*). Spectrophotometric assays were performed with a Perkin-Elmer Lamda 14 UV−vis spectrophotometer at 278 nm (ϵ_{278} = 2000 M^{-1} cm^{-1} for the enol tautomer of HK-H 1-P). Reaction mixtures (200 μL) contained 0.1−5 mM DK-H 1-P, 5 mM $MgCl_2$, 25 mM $NaHCO_3$, and 25 mM potassium HEPES (pH 7.5). Enzyme concentrations ranged from 0.1 to 10 μM. Assays for evaluating the requirement for a carboxylated active site Lys were performed without the addition of $NaHCO_3$ to the assay.

Crystallization and Data Collection. Four different crystal forms (Table 1) were grown by the hanging drop method at room temperature: (1) selenomethionine (SeMet)-substituted "enolase", (2) wild-type "enolase" and Mg^{2+}, (3) wild-type "enolase," Mg^{2+}, and HCO_3^-, and (4) wild-type "enolase," Mg^{2+}, and the stable alternate substrate DK-H 1-P. The crystallization conditions utilized the following conditions.

(1) For SeMet-substituted "enolase", the protein solution contained SeMet-substituted "enolase" from *G. kaustophilus* (11.2 mg/mL) in 20 mM Tris-HCl (pH 7.9), 100 mM NaCl, and 5 mM $MgCl_2$; the precipitant contained 1.4 M Na/K phosphate (pH 7.5). Crystals appeared in 6 days and exhibited diffraction consistent with space group $P3_221$, with two molecules of "enolase" per asymmetric unit.

(2) For "enolase" and Mg^{2+}, the protein solution contained "enolase" (14.8 mg/mL) in 20 mM Tris-HCl (pH 7.9), 100 mM NaCl, 10 mM $MgCl_2$, and 1 mM $NaHCO_3$; the precipitant contained 24% PEG 3350, 0.1 M Tris-HCl (pH 8.5), and 0.2 M ammonium acetate. For this and the remaining samples, crystals appeared in 3 days and exhibited a diffraction pattern consistent with space group $C2$, with two molecules of "enolase" per asymmetric unit.

(3) For "enolase," Mg^{2+}, and HCO_3^-, the protein solution contained "enolase" (13.0 mg/mL) in 20 mM Tris-HCl (pH 7.9), 100 mM NaCl, 10 mM $MgCl_2$, and 5 mM $NaHCO_3$; the precipitant contained 25% PEG 3350 and 0.1 M HEPES (pH 7.5).

(4) For "enolase," Mg^{2+}, and the stable alternate substrate DK-H 1-P, the protein solution contained "enolase" (15 mg/mL) in 20 mM Tris-HCl (pH 7.9), 100 mM NaCl, 10 mM $MgCl_2$, 1 mM $NaHCO_3$, and 40 mM DK-H 1-P; the precipitant contained 25% PEG 3350, 0.1 M HEPES (pH 7.5), and 0.2 M ammonium acetate.

Prior to data collection, the crystals were transferred to cryoprotectant solutions composed of their mother liquids and 20% glycerol. After incubation for ~10 s, the crystals were flash-cooled in a nitrogen stream. A one-wavelength single anomalous dispersion (SAD) data set for a crystal of SeMet-substituted "enolase" (Table 1, column 1) was collected to 2.55 Å resolution at the NSLS X9A beamline (Brookhaven National Laboratory) on a MarCCD-165 detector. Data sets for the complexes with Mg^{2+} (column 2), Mg^{2+} and HCO_3^- (column 3), and Mg^{2+} and DK-H 1-P (column 4) were collected at the NSLS X4A beamline on an ADSC CCD detector to 1.8, 1.8, and 1.7 Å resolution, respectively. Diffraction intensities were integrated and scaled with DENZO and SCALEPACK (*21*). The data collection statistics are given in Table 1.

Structure Determination and Refinement. Initial attempts to determine the structure of the "enolase" by molecular replacement using the structure of the RLP from *Chlorobium tepidum* (PDB entry 1TEL) as a search model were unsuccessful. Instead, the structure of the SeMet-substituted

"enolase" was determined by SAD with SOLVE (*22*); eight of the 10 selenium sites were identified. These heavy atom sites were used to calculate initial phases which were improved by solvent flattening and NCS averaging with RESOLVE (*23*), yielding an interpretable map for two monomers in the asymmetric unit for space group $P3_221$. Iterative cycles of manual rebuilding with TOM (*24*) and refinement with CNS (*25*) resulted in a model at 2.55 Å resolution with an R_{cryst} of 0.237 and an R_{free} of 0.245. The two polypeptides were assembled as a tight dimer. In both polypeptides, the N-terminal Met and residues 304−308 in the L6 loop at the end of the sixth β-strand in the $(\beta/\alpha)_8$-barrel domain were missing in the electron density maps. The active sites did not contain either Mg^{2+} or carboxylated Lys 173 residues. Phosphate was included in the precipitant, and a phosphate ion was hydrogen-bonded to the backbone amide groups of Gly 381, Gly 403, and Gly 404 at the ends of the seventh and eighth β-strands in sites analogous to those occupied by the 1-phosphate group of 2CABP in its complex with spinach RuBisCO (PDB entry 8RUC).

The structure of the "enolase" crystallized with Mg^{2+} was determined by molecular replacement with PHASER (*26*), using the SeMet-substituted "enolase" structure as the search model. Iterative cycles of automatic rebuilding with ARP (*27*), manual rebuilding with TOM, and refinement with CNS were performed. The model was refined at 1.8 Å with an R_{cryst} of 0.184 and an R_{free} of 0.207. A Mg^{2+} was clearly visible in the electron density maps for both polypeptides of the dimer; these were located close to Mg^{2+} binding sites in spinach RuBisCO (PDB entry 8RUC). Lys 173 was carboxylated in each polypeptide and a ligand for the Mg^{2+} ion.

The structure of the "enolase" crystallized with Mg^{2+} and HCO_3^- was determined by molecular replacement using the previous structure as the search model. Iterative cycles of automatic rebuilding with ARP, manual rebuilding with TOM, and refinement with CNS were performed. The model was refined at 1.8 Å with an R_{cryst} of 0.196 and an R_{free} of 0.220. This structure had clearly visible Mg^{2+} ions and carboxylated Lys 173 residues in both polypeptides as well as a HCO_3^- ion bound close to the phosphate binding site at the ends of the seventh and eighth β-strands in the $(\beta/\alpha)_8$-barrel domain in each polypeptide, with hydrogen bonds to the backbone amide groups of Gly 337, Gly 338, and Gly 361. The L6 loops at the ends of the sixth β-strands were ordered in both polypeptides.

The structure of the "enolase" crystallized with Mg^{2+} and DK-H 1-P was also determined by molecular replacement using the "enolase" crystallized with Mg^{2+} as the search model. The model was refined at 1.7 Å with an R_{cryst} of 0.191 and an R_{free} of 0.209. The alternate substrate DK-H 1-P was well-defined in one polypeptide and partially disordered in the second polypeptide, with only the phosphate group and C1 included in the final refined model. The structure also contained well-defined Mg^{2+} ions and carboxylated Lys 173 residues in both polypeptides. Again, the L6 loops at the ends of the sixth β-strands were ordered in both polypeptides.

Final refinement statistics for all four structures are given in Table 1.

Scheme 1

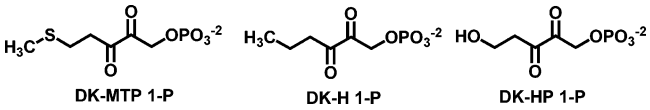

RESULTS AND DISCUSSION

Although attempts to crystallize the "enolase" from *B. subtilis* were not successful (*7*), we were able to determine the structure of the "enolase" from *G. kaustophilus*. Our experimental strategy was to restrict the location of the general base by determining the stereochemical course of the proton abstraction reaction. With the three-dimensional structure, we then would be able to identify the general base.

Methionine Salvage Pathway Enzymes from B. subtilis Utilize D*-Ribose Derivatives.* The natural substrate for the "enolase," DK-MTP 1-P, is susceptible to elimination of methanethiol (*1*, *7*, *20*); the structures of the substrates for the "enolase" used in our studies are shown in Scheme 1.

2,3-Diketohexane 1-phosphate (DK-H 1-P), a stable desthio alternate substrate, is used to quantitate the activity of the "enolase", because formation of the enol product is accompanied by an increase in absorbance at 278 nm (*1*, *20*). Although we also used DK-H 1-P in our crystallographic studies, it cannot be readily stereospecifically labeled with deuterium at C1 for stereochemical studies.

We determined that D-ribose (differs from MTR by the substitution of the 5-SCH_3 group with a 5-OH group) and downstream pathway derivatives are substrates for the enzymes in the methionine salvage pathway (Scheme 2). D-Ribose deuterated at either C1 or C2 can be purchased, so we envisaged a strategy for synthesizing chirally deuterated samples of D-ribulose 1-phosphate. These, in turn, could be converted to the DK-HP 1-P substrate so that stereochemical studies could be performed.

DK-HP 1-P was presented to the "enolases" from *G. kaustophilus* and *B. subtilis*; the products were analyzed by ^1H NMR spectroscopy. In each reaction, the spectrum of the HK-HP 1-P product contained a vinyl doublet indicative of coupling of the single proton on C1 of the tautomerized product to the 1-phosphate group (*B. subtilis*, Figure 4A; *G.*

Scheme 2

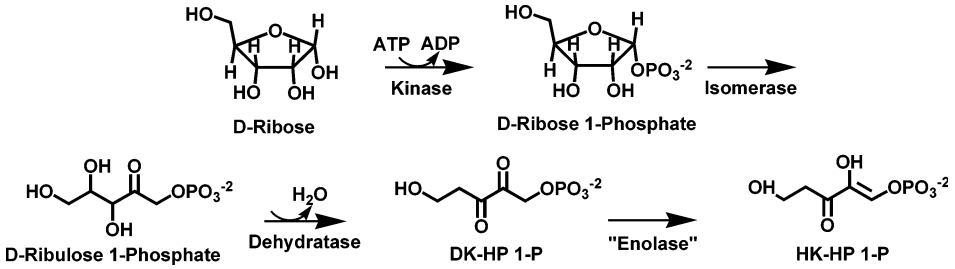

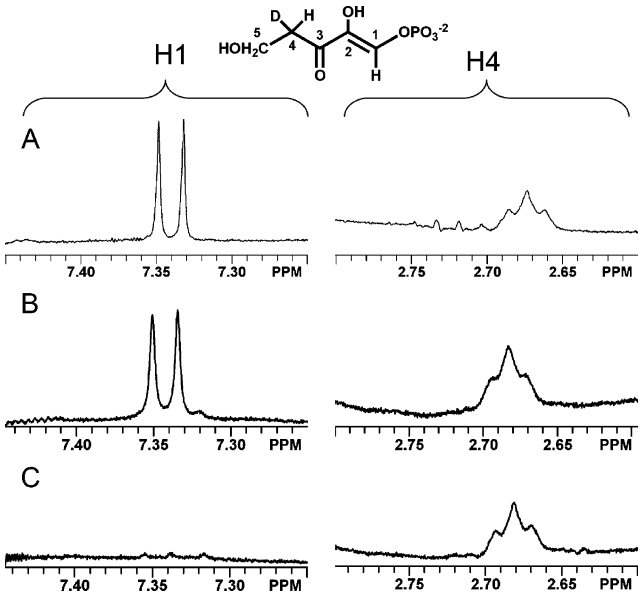

FIGURE 4: ^{1}H NMR spectra of samples of HK-HP 1-P produced by the action of the "enolase" from *B. subtilis* on samples of DK-HP 1-P generated in situ from samples of D-ribulose 1-phosphate. (A) Partial ^{1}H NMR spectrum of unlabeled HK-HP 1-P from unlabeled ribulose 1-P, (B) [1*S*-^{2}H]-D-ribulose 1-P, and (C) [1*R*-^{2}H]-D-ribulose 1-P.

Scheme 3

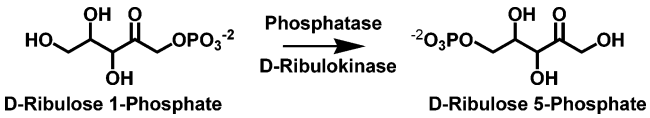

kaustophilus, data not shown). Each spectrum also contained a broad triplet associated with a single proton on C4 (a single deuteron is also located on C4 as the result of the dehydration and ketonization) as well as a doublet for the methylene group of C5.

MTR 1-P Isomerase Catalyzes Stereospecific Proton Transfer. Because the product of the isomerase-catalyzed reaction from α-D-ribose 1-P is D-ribulose 1-phosphate, we recognized that the configurations of deuteriated samples could be determined following a two step "mutase" reaction in which [1-^{2}H]-D-ribulose 1-phosphate is converted to [1-^{2}H]-D-ribulose 5-phosphate (alkaline phosphatase followed by D-ribulokinase; Scheme 3). Previous studies in our laboratory had assigned the resonances of the C1 protons of D-ribulose 5-phosphate (*17*). Because the dehydratase-catalyzed reaction does not alter the configuration of C1, the assignment of the configuration of [1-^{2}H]-D-ribulose 1-phosphate assigns the configuration of the 1-^{2}H-labeled substrate for the "enolase".

D-Ribulose 1-phosphate has a complex ^{1}H spectrum consistent with the presence of the α- and *β*-anomers of its hemiketal (Figure 5A,B). Using the successive actions of the kinase and isomerase, both [1-^{2}H]-D-ribose and [2-^{2}H]-D-ribose were converted to samples of [1-^{2}H]-D-ribulose 1-phosphate. Although the ^{1}H NMR spectra of the products are congested in the region that contains the resonances associated with the protons on C1, they are consistent with complementary labeling of the hydrogens with deuterium (Figure 5C,D).

The [1-^{2}H]-D-ribulose 1-phosphate obtained from [1-^{2}H]-D-ribose was subjected to the successive actions of calf

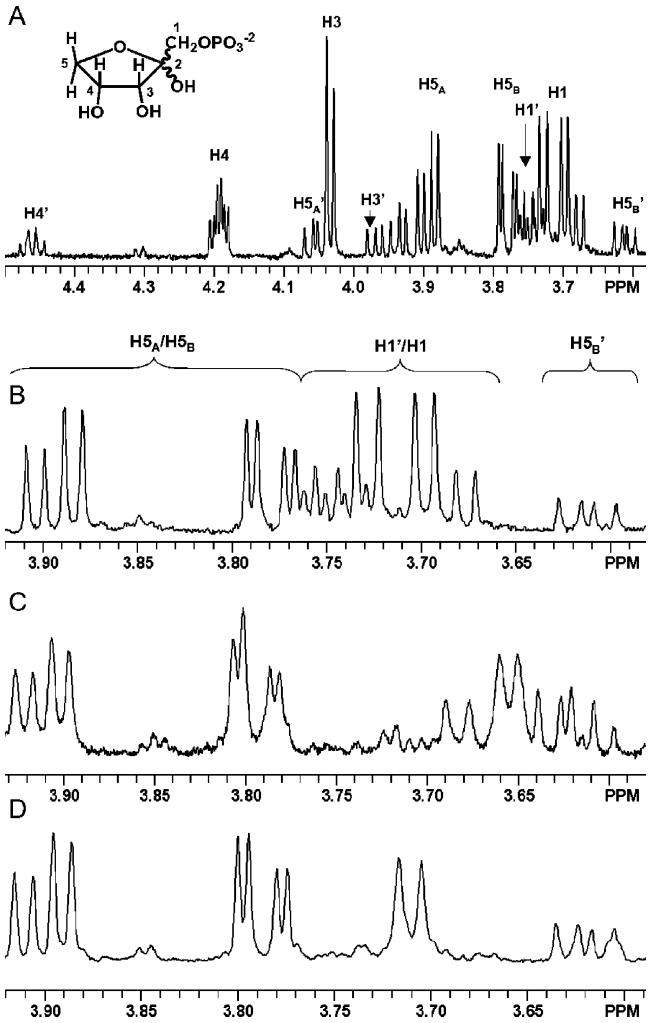

FIGURE 5: ^{1}H NMR spectra of samples of D-ribulose 1-P produced by the action of MTRu 1-P isomerase on D-ribose 1-P. (A) ^{1}H NMR spectrum of unlabeled D-ribulose 1-P showing assignments of all protons. (B) Partial ^{1}H NMR spectrum of unlabeled D-ribulose 1-P. (C) Partial ^{1}H NMR spectrum of [1*S*-^{2}H]-D-ribulose 1-P obtained from [1-^{2}H]-D-ribose. (D) Partial ^{1}H NMR spectrum of [1*R*-^{2}H]-D-ribulose 1-P obtained from [2-^{2}H]-D-ribose.

intestinal alkaline phosphatase and D-ribulokinase. The resulting ^{1}H NMR spectrum matched that of a spectrum of [1*S*-^{2}H]-D-ribulose 5-phosphate previously published by our laboratory (Figure 6B; panel A is a spectrum of unlabeled D-ribulose 5-phosphate) (*17*), establishing the stereochemical course of the isomerase-catalyzed reaction as well as the stereochemical identity of the product. Thus, we assign the 1*S* configuration to the sample of the [1-^{2}H]-D-ribulose 1-phosphate obtained from [1-^{2}H]-D-ribose 1-phosphate.

We attempted the complementary "mutase" reactions with the [1-^{2}H]-D-ribulose 1-phosphate obtained from [2-^{2}H]-D-ribose. In this case, although the [1-^{2}H]-D-ribulose 1-phosphate was stereospecifically labeled with deuterium (Figure 5D), the resulting D-ribulose 5-phosphate was a mixture of unlabeled D-ribulose 5-phosphate and [1*R*-^{2}H]-D-ribulose 5-phosphate (Figure 6C). We attribute the partial exchange of the deuterium with solvent protium to either incomplete removal of the isomerase by ultrafiltration or a contamination of the D-ribulokinase with D-ribose isomerase (the "mutase" sequence is conducted in H_2O-containing solutions). On the basis of the complementary ^{1}H NMR spectra obtained for the samples of [1-^{2}H]-D-ribulose 1-phos-

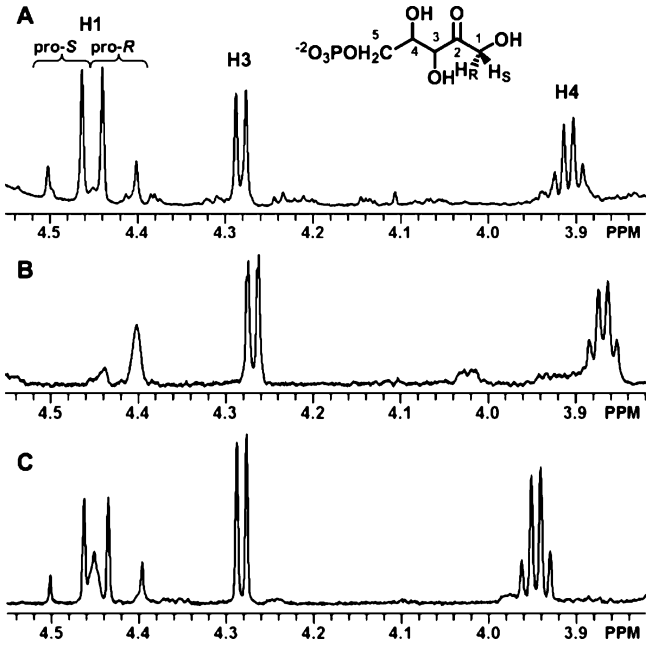

FIGURE 6: ^{1}H NMR spectra of samples of D-ribulose 5-phosphate obtained by the successive actions of calf intestinal alkaline phosphatase and D-ribulokinase. (A) Unlabeled D-ribulose 5-phosphate from unlabeled D-ribulose 1-P. (B) [1*S*-^{2}H]-D-Ribulose 5-P from [1*S*-^{2}H]-D-ribulose 1-P. (C) [1*R*-^{2}H]-D-Ribulose 5-P from [1*R*-^{2}H]-D-ribulose 1-P.

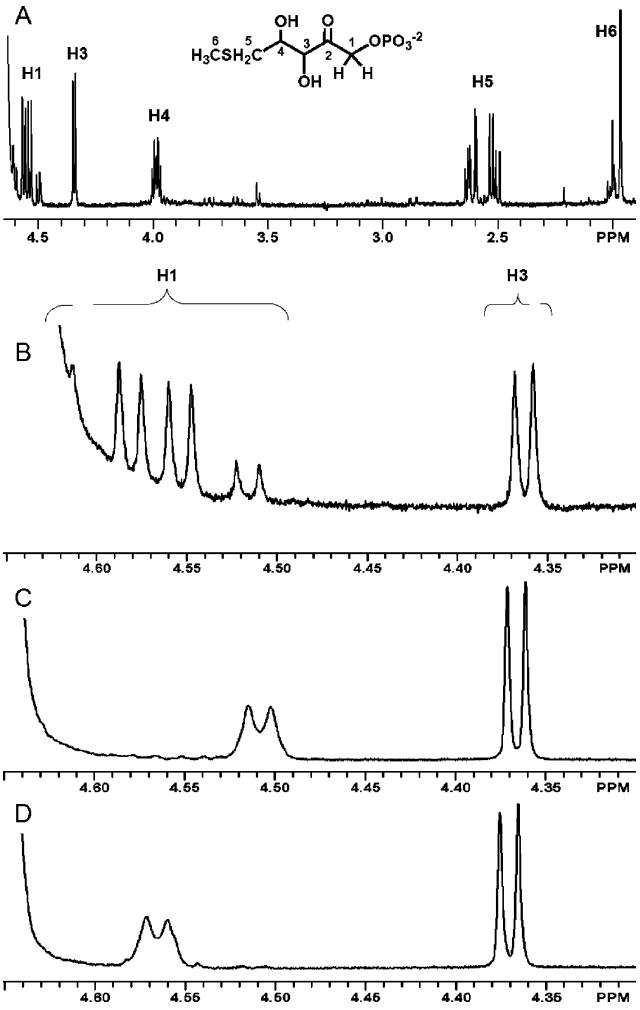

FIGURE 7: ^{1}H NMR spectra of samples of 5-methylthio-D-ribulose 1-phosphate. (A) Unlabeled 5-methylthio-D-ribulose 1-P showing assignments of all protons. (B) Partial ^{1}H NMR spectrum of unlabeled 5-methylthio-D-ribulose 1-phosphate. (C) Partial ^{1}H NMR spectrum of [1*S*-^{2}H]-5-methylthio-D-ribulose 1-phosphate. (D) Partial ^{1}H NMR spectrum of [1*R*-^{2}H]-5-methylthio-D-ribulose 1-phosphate.

phate obtained from [1-^{2}H]-D-ribose and [2-^{2}H]-D-ribose, we assign the 1*R* configuration to the sample of [1-^{2}H]-D-ribulose 1-phosphate obtained from [2-^{2}H]-D-ribose.

"Enolases" Catalyze Abstraction of the 1-proS Hydrogen from DK-HP 1P, the D-Ribose-Derived Substrate. [1*S*-^{2}H]-D-Ribulose 1-phosphate was incubated with a limiting amount of dehydratase and an excess of the "enolase" from either *B. subtilis* or *G. kaustophilus* to prevent the accumulation of DK-HP 1-P. A downfield phosphorus-coupled doublet associated with the hydrogen on C1 of the HK-HP 1-P product appeared along with resonances associated with the hydrogens on C4 and C5. The vinyl and C4 proton resonances each are associated with a single proton, so the latter resonance provides an integration standard for determining the extent of loss of deuterium from C1 in the "enolase" reaction.

Using the "enolase" from *B. subtilis*, the integration ratio was 1.06:1.00 (C1:C4), demonstrating that the deuterium had been abstracted (Figure 4B). When [1*R*-^{2}H]-D-ribulose 1-phosphate was used as the substrate in the complementary experiment, the downfield phosphorus-coupled doublet was barely visible, although the resonances associated with the hydrogens on C4 and C5 signals were present (Figure 4C). Integration resulted in a ratio of 0.05:1.00 (C1:C4), demonstrating that the protium had been abstracted. The observations demonstrate that the "enolase" from *B. subtilis* catalyzes abstraction of the 1-*proS* proton of the DK-HP 1-P substrate. Similar results were obtained with the "enolase" from *G. kaustophilus* (data not shown).

"Enolases" Catalyze Abstraction of the 1-proS Hydrogen of DK-MTP 1-P, the Natural Substrate. Although our stereochemical experiments using samples of D-ribose-derived DK-HP 1-P provide compelling evidence that the "enolases" abstract the 1-*proS* hydrogen, we also determined the stereochemical course using natural MTR-derived substrates.

We assumed that the stereochemical course of the isomerase reaction would not be altered by the identity of the functional group on C5 of its substrate (a 5-OH group for the D-ribose-derived substrate and a 5-SCH_3 group for the MTR-derived substrate). We prepared samples of MTR from [1-^{2}H]-D-ribose and [2-^{2}H]-D-ribose as described in Materials and Methods. These were enzymatically phosphorylated and isomerized to obtain two samples of MTRu 1-P. As shown by the ^{1}H NMR spectra presented in Figure 7, these were stereospecifically labeled with deuterium. Panels A and B display spectra of unlabeled MTRu 1-P. On the basis of the stereochemical course of the isomerase determined with the D-ribose substrates, we assign the sample obtained from [1-^{2}H]-D-ribose as [1*S*-^{2}H]-MTRu 1-P (panel C) and the sample obtained from [1-^{2}H]-D-ribose as [1*R*-^{2}H]-MTRu 1-P (panel D).

When these samples of deuterated MTRu 1-P were incubated with a limiting amount of dehydratase and excess "enolase" from either *B. subtilis* or *G. kaustophilus*, the results were as expected on the basis of the experiments using

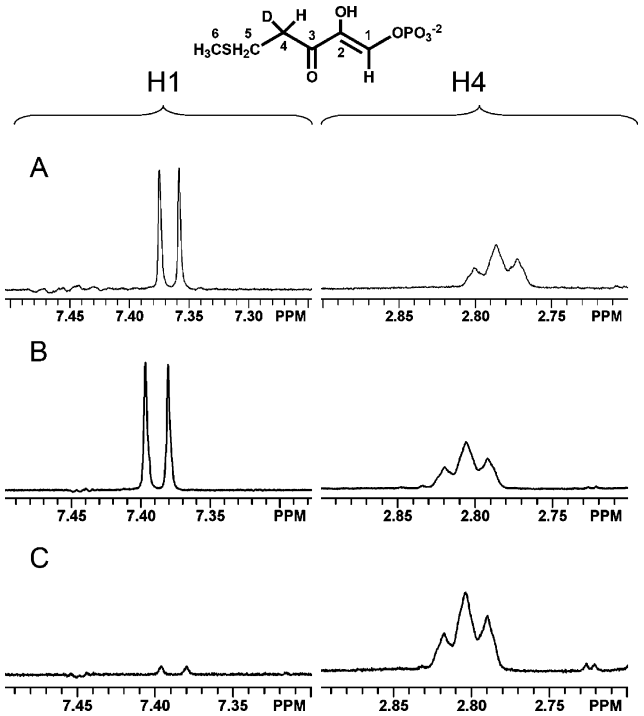

FIGURE 8: ^{1}H NMR spectra of samples of HK-MTP 1-P produced by the action of the "enolase" from *G. kaustophilus* on samples of DK-MTP 1-P generated in situ from samples of MTRu 1-P. (A) Partial ^{1}H NMR spectrum of unlabeled HK-MTP 1-P from unlabeled MTRu 1-P. (B) Partial ^{1}H NMR spectrum of HK-MTP 1-P from [1*S*-^{2}H]-MTRu 1-P. (C) Partial ^{1}H NMR spectrum of HK-MTP 1-P from [1*R*-^{2}H]-MTRu 1-P.

the D-ribose-derived alternate substrate (Figure 8, "enolase" from *G. kaustophilus*). Panel A displays the spectrum of the HK-MTP 1-P product obtained from unlabeled MTRu 1-P. If we started with [1*S*-^{2}H]-MTRu 1-P, the proton was retained; the ratio of the integration of the resonance associated with the enol proton to that associated with the C4 proton was 0.86:1.00 (C1:C4) (Figure 8B). If we start with [1*R*-^{2}H]-MTRu 1-P, the deuteron was retained; the ratio of the integration of the resonances associated with the enol proton to that associated with the C4 proton was 0.03:1.00 (C1:C4) (Figure 8C). Similar results were obtained for the "enolase" from *B. subtilis* (data not shown). These results demonstrate that the 1-*proS* proton is stereospecifically abstracted from the natural DK-MTP 1-P substrate.

Thus, whether we used the stereospecifically deuterated substrates derived from D-ribose or MTR, the stereochemical course of the "enolase" reaction is the same: the 1-*proS* hydrogen is abstracted from the 2,3-diketo substrate.

Carboxylation of Lys 173. The "enolases" contain the same Mg^{2+}-binding motif, KDDE, found in RuBisCOs (Figure 3); in the "enolase" from *G. kaustophilus*, Lys 173, Asp 174, Asp 175, and Glu 176 are located at the end of the second β-stand in the C-terminal $(\beta/\alpha)_8$-barrel domain. In RuBisCOs, the Lys in this motif is carboxylated to allow it to serve both as a ligand for the Mg^{2+} that stabilizes the enolate anion intermediate and as the general base that initiates the carboxylation reaction by abstraction of a proton from C3.

We probed the importance of carboxylation by determining whether the reaction is activated by sodium bicarbonate. Using the stable alternate showed that the k_{cat}/K_M for DK-H 1-P using the "enolase" from *G. kaustophilus* is 200 M^{-1} s^{-1} after preincubation with sodium bicarbonate as compared

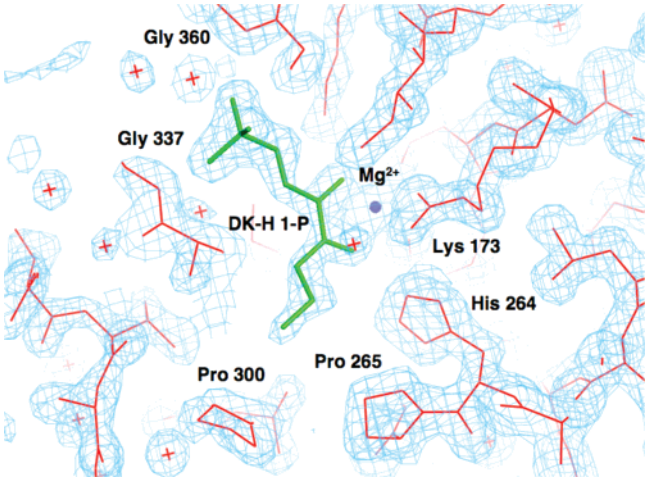

FIGURE 9: Representative electron density for the active site of the "enolase" activated with bicarbonate and complexed with Mg^{2+} and the alternate substrate DK-H 1-P (structure **4**). The details of the interactions between the alternate substrate and active site are described in the text.

to 130 M^{-1} s^{-1} without preincubation. Partial activity is common for RuBisCOs and is attributed to a contaminating bicarbonate present in buffers (*28*). As described in a subsequent section, when the "enolase" is crystallized in the presence of bicarbonate, Lys 173 is carboxylated. We conclude that Lys 173 is carboxylated in the "enolases".

Structure of the "Enolase" from G. kaustophilus. We determined four structures of the "enolase" from *G. kaustophilus* (Table 1): (1) SeMet-labeled protein complexed with inorganic phosphate (structure **1**; 2OEJ), (2) wild-type protein activated with bicarbonate and complexed with Mg^{2+} (structure **2**; 2OEK), (3) activated wild-type protein complexed with Mg^{2+} and bicarbonate (structure **3**; 2OEL), and (4) activated wild-type protein complexed with Mg^{2+} and DK-H 1-P (structure **4**; 2OEM), the desthio alternate substrate (Scheme 1). Representative electron density for the active site region in structure **4** is shown in Figure 9.

The polypeptide of the "enolase", like the polypeptide of RuBisCO, is composed of two domains, an N-terminal $\alpha+\beta$ domain (residues 1−120) and a C-terminal $(\beta/\alpha)_8$-barrel domain (residues 121−413). The polypeptides are packed as tight dimers, as found in the structure of RuBisCO; the active sites (two per dimer) are located at the interfaces between the N-terminal domain of one polypeptide and the C-terminal face of the (β/α)-barrel of the second polypeptide. The structures of the dimers of the "enolase" and RuBisCO are compared in Figure 10 (panel A, "enolase"; panel B, spinach RuBisCO); the arrows mark the locations of the active sites. Descriptions of the secondary structural elements and the dimer interface are provided in the Supporting Information.

Structure of the Active Site. The active sites of the "enolase" complexed with the alternate substrate DK-H 1-P and of RuBisCO complexed with intermediate analogue 2CABP are compared in Figure 11 (panels A and B, respectively).

In three structures (**2**−**4**), Lys 173 is carboxylated. In RuBisCO, the homologous Lys 201 is also carboxylated, and a carbamate oxygen is the general base that abstracts the

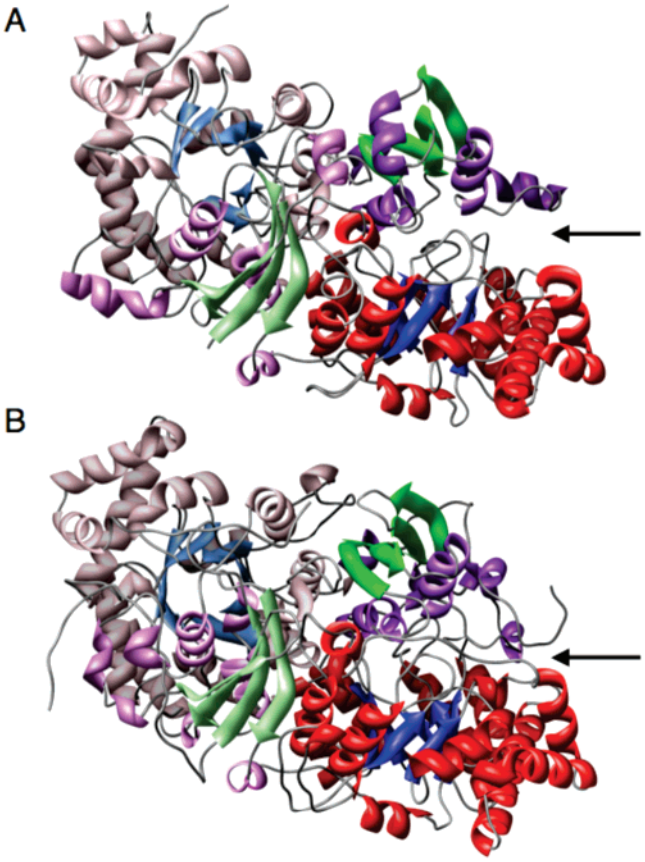

FIGURE 10: (A) Dimer structure of the "enolase" from *G. kaustophilus*. (B) Dimer structure of the RuBisCO from spinach (8RUC). In the first polypeptide in each dimer, the α-helices and *β*-strands in the N-terminal α+*β* domain are colored light purple and light green, respectively; the α-helices and *β*-strands in the C-terminal $(\beta/\alpha)_8$-barrel domain are colored red and blue, respectively. In the second polypeptide, the α-helices and *β*-strands in the N-terminal α+*β* domain are colored purple and green, respectively; the α-helices and *β*-strands in the C-terminal $(\beta/\alpha)_8$-barrel domain are colored pink and light blue, respectively. The position of the active site at the interface of the C-terminal $(\beta/\alpha)_8$-barrel domain of the first polypeptide and the N-terminal α+*β* domain of the second polypeptide in each dimer is marked with an arrow.

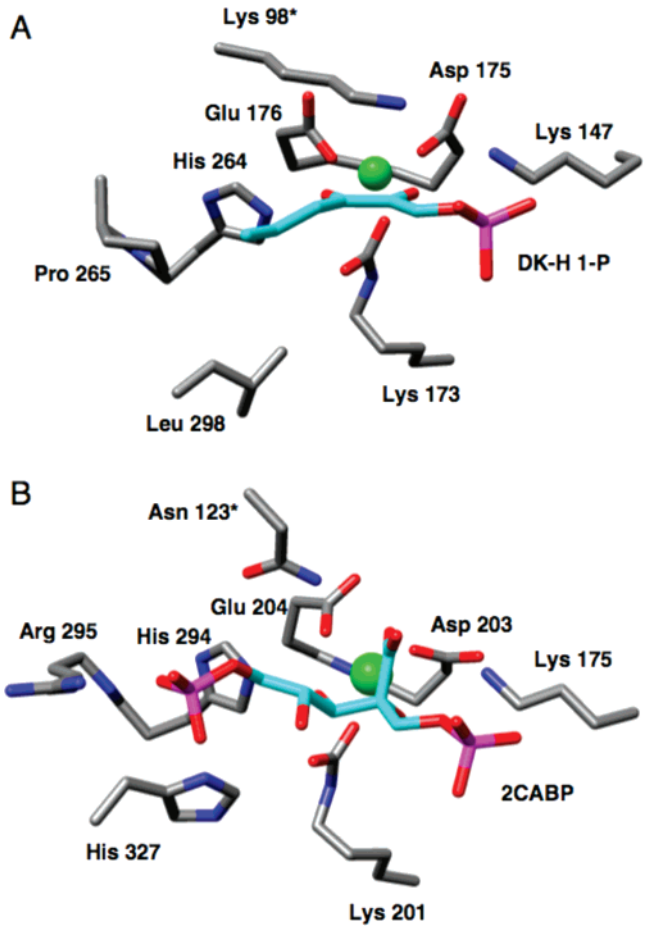

FIGURE 11: Comparison of the active sites of the "enolase" from *G. kaustophilus* complexed with Mg^{2+} and DK-H 1-P (A) and the RuBisCO from spinach complexed with Mg^{2+} and 2-CABP (B). Key pairs of residues that are conserved or diverged are shown; their importance is described in the text.

proton from C3 of the D-ribulose 1,5-bisphosphate substrate.

The side chain of the carboxylated Lys 173 adopts the same conformation as that of the homologous carboxylated Lys 201 in RuBisCO. One oxygen of the carbamate group is coordinated to the Mg^{2+}; the second oxygen is hydrogen-bonded to His 264, O3 of the alternate substrate, and a water molecule. The Mg^{2+} ion is also coordinated to carboxylate oxygens of Asp 175 and Glu 176. In structures determined in the absence of a ligand (structure **2**) and in the presence of bicarbonate (structure **3**), two water molecules are coordinated to the Mg^{2+}. In the structure determined in the presence of the alternate substrate (structure **4**), the water molecules are replaced by the oxygens of C2 and C3 from the ligand (vide infra). This metal ion coordination is analogous to that in RuBisCO where it involves Asp 203, Glu 204, and the carboxylated Lys 201 (*29*).

In the structure obtained with the alternate substrate, one active site contains electron density for the entire ligand (Figure 11A); the second active site contains electron density for only C1 and the phosphate group. The binding of the alternate substrate is accompanied by several changes in the conformation of the active site. The L6 and L7 loops at the ends of the sixth and seventh *β*-strands move closer to the substrate with displacements of ∼2 Å for their Cα atoms. The conformation of the L8 loop at the end of the eighth *β*-strand is also altered with a maximum displacement of 2.7 Å for the Cα atom of Gly 361 between the liganded and unliganded forms.

The oxygens of C2 and C3 of the ligand are oriented in a cis conformation so that both can coordinate to the Mg^{2+}. The oxygen of C2 is also hydrogen bonded to Lys 147, Asp 175, a carbamate oxygen of carboxylated Lys 173, and a water molecule; the oxygen of C3 is also hydrogen bonded to Glu 176, His 264, a carbamate oxygen of carboxylated Lys 173, and a water molecule. The hydroxyl groups of C2 and C3 of the 2CABP intermediate analogue also are found in a cis conformation so that they also can coordinate to the Mg^{2+} in the active site of RuBisCO. Thus, as in RuBisCO, the 2-keto group of the substrate for the "enolase" is coordinated to the Mg^{2+} so that the enolate anion derived from proton abstraction from C1 can be stabilized.

The phosphate oxygens of the alternate substrate form hydrogen bonds to the backbone amide groups of Gly 337, Gly 359, and Gly 360 as well as three water molecules. This

binding site is identical to the P1 phosphate site in RuBisCO, formed by the backbone amide groups of Gly 381, Gly 403, and Gly 404. In the "enolase", phosphate O1 of DK-H 1-P forms a hydrogen bond to Lys 147; in RuBisCO, the phosphate O1 of 2CABP forms an analogous hydrogen bond to conserved Lys 175.

The alternate substrate is bound in an extended conformation similar to that observed for 2CABP in RuBisCO. The P1 phosphate and the carbon backbone of DK-H 1-P in the "enolase" occupy positions similar to those of the P1 phosphate and C1, C2, C3, C4, C5, and O5 of 2CABP in RuBisCO. In the complex of 2CABP with RuBisCO, the C4 hydroxyl group is hydrogen-bonded to Ser 379; although the natural DK-MTP 1-P substrate lacks an analogue of this hydroxyl group, Ser 335 is conserved. In RuBisCO, the 5-phosphate group of 2CABP is hydrogen-bonded to Arg 295 and His 327; in the "enolase", C5 and C6 are located in a hydrophobic pocket formed by Pro 265, Leu 298, Pro 300, and Ala 336 from one polypeptide and Leu 101 from the N-terminal domain of the second polypeptide. This hydrophobic pocket would accommodate the 5-methythio group of the natural DK-MTP 1-P substrate.

In RuBisCO, the 2′-carboxyl group of the 2CABP molecule is hydrogen-bonded to Lys 177 and Lys 334 in the L6 loop and Asn 123 in the symmetry-related polypeptide, with the latter interaction stabilizing the transition state for carboxylation. In the "enolase", Met 149 is the homologue of Lys 177 in RuBisCO, residues in the L6 loop do not interact with the bound alternate substrate, and Lys 98 in the αC helix of the symmetry-related peptide (the homologue of Asn 123 in RuBisCO) is located 3.4 Å from C1 in the alternate substrate.

Lysine 98 Is the General Base. In addition to the carboxylated Lys 173, the active site of the "enolase" contains conserved homologues of two additional acid−base catalysts that have been implicated in the RuBisCO reaction (Figure 11A): Lys 147 (Lys 175 in RuBisCO protonates the molecule of 3-phosphoglycerate derived from C1 and C2 of the substrate) and His 264 (His 294 in RuBisCO functions as the general base for attack of water on C3 of the carboxylated intermediate).

The ϵ-amino group of Lys 147, located at the C-terminal end of the first β-strand in the $(\beta/\alpha)_8$-barrel domain, is both too far from C1 (4.0 Å) and improperly positioned to abstract the 1-*proS* proton from the alternate substrate. Lys 147 is hydrogen-bonded to the oxygens of C2 and C3 of the alternate substrate, thereby reinforcing the orientation of the substrate in the active site.

His 264 is hydrogen-bonded to the keto oxygen of C3 of the alternate substrate; the closest carbon is C4 (4.1 Å). His 294 also is not positioned to abstract the 1-*proS* proton from the substrate.

The carbamate group of carboxylated Lys 173 also is too far from (4.4 Å) and located on the *re* face of C1 of the alternate substrate, thereby preventing it from abstracting the 1-*proS* proton from the substrate.

However, the ϵ-amino group of Lys 98, conserved in all "enolases", is located 3.4 Å from the *si* face of C1 of the alternate substrate, the face derived from abstraction of the 1-*proS* proton. Therefore, Lys 98 is appropriately positioned to be the general base.

Thus, from both the identity of the abstracted proton (1-*proS*) and the geometry of the complex between the "enolase" and the alternate substrate, we deduce that Lys 98 is the only candidate for the general base in the "enolase"-catalyzed reaction.

Site-Directed Mutagenesis of Active Site Residues. To test this conclusion, we constructed Ala substitutions for Lys 98, Lys 147, and Lys 173. Each mutant protein was assayed for "enolase" activity with the spectrophotometric assay using the desthio DK-H 1-P alternate substrate and also with ^{1}H NMR spectroscopy to observe formation of the enolized product from DK-MTP 1-P (generated in situ from MTR 1-P). Using the spectrophotometric assay, only the K173A mutant had any detectable activity, ∼3% of that of the wild-type "enolase". These assays were performed with elevated (10 μM) concentrations of the mutant enzymes; because the λ_{max} of enolized product is 278 nm, the assay is limited to "low" enzyme concentrations.

Using the natural substrate and ^{1}H NMR spectroscopy, the K173A mutant was able to catalyze enolization at approximately the same rate as the wild-type enzyme (using 10 μM protein, data not shown). Because this mutant retains two ligands for the essential Mg^{2+} (Asp 175 and Glu 176), the observed activity likely reflects the ability of the active site to bind the Mg^{2+} and stabilize the enolate anion intermediate derived by abstraction of the 1-*proS* proton from the substrate. That the K173A mutant also retains some ability to enolize the desthio substrate provides persuasive evidence that the carboxylated Lys 173 is not the general base in the "enolase"-catalyzed reaction, although the carboxylated Lys 201 in spinach RuBisCO is the general base that initiates the carboxylation reaction.

The K147A mutant required a 10-fold greater concentration of protein (100 μM) for observation of enolization of the natural substrate (data not shown). That this mutant retained catalytic activity is persuasive evidence that it, also, is not the general base. However, no enolization of the natural substrate could be observed with the K98A mutant, even at a protein concentration of 150 μM (data not shown).

With this result, along with stereochemical information, we conclude that Lys 98 is the general base in the "enolase"-catalyzed reaction. In addition, Lys 98 is absolutely conserved in the "enolases", and as noted previously, in RuBisCOs the residue homologous to Lys 98 is Asn 123. Although Asn 123 does not function as an acid−base catalyst in the RuBisCO-catalyzed reaction, it is located so that it can stabilize the transition state for carboxylation which occurs on the homologous face of the substrate (Figure 11).

Conclusions. Our stereochemical studies together with the structure of the "enolase" from *G. kaustophilus* provide compelling evidence that Lys 98 is the general base. Thus, the divergent evolution of function in the RuBisCO superfamily utilizes a conserved structural strategy for stabilizing an enolate anion intermediate by coordination to a Mg^{2+} ion but allows different structural strategies for abstraction of a proton from the substrate to initiate the reaction. We note that divergent evolution of the function in the mechanistically diverse enolase superfamily uses the same principles (*4*).

We expect that RLPs of currently unknown function will also catalyze reactions that are initiated by enolization and/or tautomerization of ketose 1-phosphate substrates. For

example, in the orthologous group of RLPs that includes the structurally characterized protein from *C. tepidum* (A. A. Fedorov, H. J. Imker, E. V. Fedorov, J. A. Gerlt, and S. C. Almo, unpublished structure, deposited as PDB entry 1TEL October 5, 2004; see also ref *9*), a Glu is the homologous residue of Lys 98 in the "enolases". Although the substrate for this protein is unknown, the presence of the carbamate group of the carboxylated Lys residue in the C-terminal $(\beta/\alpha)_8$-barrel domain and the Glu in the N-terminal $\alpha+\beta$ domain on opposite faces of the active site suggest that this protein could catalyze the epimerization of C3 in an unknown ketose 1-phosphate substrate. Indeed, we have observed that the RLP from *C. tepidum* catalyzes the non-stereospecific exchange of both 3-hydroxymethylene protons in dihydroxyacetone 1-phosphate (H. J. Imker and J. A. Gerlt, unpublished observations). Thus, we expect that the identification of the general base in the "enolase"-catalyzed reaction will facilitate the functional assignment of the remaining members of the RuBisCO superfamily.

ACKNOWLEDGMENT

We thank Professor Thomas Pochapsky (Brandeis University, Waltham, MA) for the generous gift of the initial sample of DK-H 1-P.

SUPPORTING INFORMATION AVAILABLE

Descriptions of the secondary structural elements of the "enolase" polypeptide and of the dimer interface. This material is available free of charge via the Internet at http://pubs.acs.org.

REFERENCES

1. Myers, R. W., Wray, J. W., Fish, S., and Abeles, R. H. (1993) Purification and characterization of an enzyme involved in oxidative carbon-carbon bond cleavage reactions in the methionine salvage pathway of *Klebsiella pneumoniae*, *J. Biol. Chem. 268*, 24785−24791.
2. Balakrishnan, R., Frohlich, M., Rahaim, P. T., Backman, K., and Yocum, R. R. (1993) Appendix. Cloning and sequence of the gene encoding enzyme E-1 from the methionine salvage pathway of *Klebsiella oxytoca*, *J. Biol. Chem. 268*, 24792−24795.
3. Babbitt, P. C., Hasson, M. S., Wedekind, J. E., Palmer, D. R., Barrett, W. C., Reed, G. H., Rayment, I., Ringe, D., Kenyon, G. L., and Gerlt, J. A. (1996) The enolase superfamily: A general strategy for enzyme-catalyzed abstraction of the α-protons of carboxylic acids, *Biochemistry 35*, 16489−16501.
4. Gerlt, J. A., Babbitt, P. C., and Rayment, I. (2005) Divergent evolution in the enolase superfamily: The interplay of mechanism and specificity, *Arch. Biochem. Biophys. 433*, 59−70.
5. Cleland, W. W., Andrews, T. J., Gutteridge, S., Hartman, F. C., and Lorimer, G. H. (1998) Mechanism of RuBisCO: The Carbamate as General Base, *Chem. Rev. 98*, 549−562.
6. Pearce, F. G., and Andrews, T. J. (2003) The relationship between side reactions and slow inhibition of ribulose-bisphosphate carboxylase revealed by a loop 6 mutant of the tobacco enzyme, *J. Biol. Chem. 278*, 32526−32536.
7. Ashida, H., Saito, Y., Kojima, C., Kobayashi, K., Ogasawara, N., and Yokota, A. (2003) A functional link between RuBisCO-like protein of *Bacillus* and photosynthetic RuBisCO, *Science 302*, 286−290.
8. Hanson, T. E., and Tabita, F. R. (2003) Insights into the stress response and sulfur metabolism revealed by proteome analysis of a *Chlorobium tepidum* mutant lacking the RuBisCO-like protein, *Photosynth. Res. 78*, 231−248.
9. Li, H., Sawaya, M. R., Tabita, F. R., and Eisenberg, D. (2005) Crystal structure of a RuBisCO-like protein from the green sulfur bacterium *Chlorobium tepidum*, *Structure 13*, 779−789.
10. Gerlt, J. A., and Babbitt, P. C. (2001) Divergent evolution of enzymatic function: Mechanistically diverse superfamilies and functionally distinct suprafamilies, *Annu. Rev. Biochem. 70*, 209−246.
11. Furfine, E. S., and Abeles, R. H. (1988) Intermediates in the conversion of 5′-S-methylthioadenosine to methionine in *Klebsiella pneumoniae*, *J. Biol. Chem. 263*, 9598−9606.
12. Avila, M. A., Garcia-Trevijano, E. R., Lu, S. C., Corrales, F. J., and Mato, J. M. (2004) Methylthioadenosine, *Int. J. Biochem. Cell Biol. 36*, 2125−2130.
13. Koonin, E. V., and Tatusov, R. L. (1994) Computer analysis of bacterial haloacid dehalogenases defines a large superfamily of hydrolases with diverse specificity. Application of an iterative approach to database search, *J. Mol. Biol. 244*, 125−132.
14. Wang, H., Pang, H., Bartlam, M., and Rao, Z. (2005) Crystal structure of human E1 enzyme and its complex with a substrate analog reveals the mechanism of its phosphatase/enolase activity, *J. Mol. Biol. 348*, 917−926.
15. Ames, B. N. (1966) Assay of inorganic phosphate, total phosphate and phosphatases, *Methods Enzymol. 8*, 115−118.
16. Avidad, G. (1975) Colorimetric ultramicro assay for reducing sugars, *Methods Enzymol. 41*, 27−29.
17. Yew, W. S., Akana, J., Wise, E. L., Rayment, I., and Gerlt, J. A. (2005) Evolution of enzymatic activities in the orotidine 5′-monophosphate decarboxylase suprafamily: Enhancing the promiscuous D-arabino-hex-3-ulose 6-phosphate synthase reaction catalyzed by 3-keto-L-gulonate 6-phosphate decarboxylase, *Biochemistry 44*, 1807−1815.
18. Van derpoorten, K., and Migaud, M. E. (2004) Isopolar phosphonate analogue of adenosine diphosphate ribose, *Org. Lett. 6*, 3461−3464.
19. Myers, R. W., and Abeles, R. H. (1990) Conversion of 5-S-methyl-5-thio-D-ribose to methionine in *Klebsiella pneumoniae*. Stable isotope incorporation studies of the terminal enzymatic reactions in the pathway, *J. Biol. Chem. 265*, 16913−16921.
20. Zhang, Y., Heinsen, M. H., Kostic, M., Pagani, G. M., Riera, T. V., Perovic, I., Hedstrom, L., Snider, B. B., and Pochapsky, T. C. (2004) Analogs of 1-phosphonooxy-2,2-dihydroxy-3-oxo-5-(methylthio)pentane, an acyclic intermediate in the methionine salvage pathway: A new preparation and characterization of activity with E1 enolase/phosphatase from *Klebsiella oxytoca*, *Bioorg. Med. Chem. 12*, 3847−3855.
21. Otwinowski, Z., and Minor, W. (1997) Processing of X-ray diffraction data collected in oscillation mode, in *Methods in Enzymology* (Carter, C. W. J., Sweet, R. M., Abelson, J. N., and Simon, M. I., Eds.) pp 307−326, Academic Pres, New York.
22. Terwilliger, T. C., and Berendzen, J. (1999) Automated MAD and MIR structure solution, *Acta Crystallogr. D55*, 849−861.
23. Terwilliger, T. C. (2000) Maximum-likelihood density modification, *Acta Crystallogr. D56*, 965−972.
24. Jones, A. T. (1985) Interactive computer graphics: FRODO, *Methods Enzymol. 115*, 157−171.
25. Brunger, A. T., Adams, P. D., Clore, G. M., DeLAno, W. L., Gros, P., Grosse-Kunstleve, R. W., Jiang, J. S., Kuszewski, J., Nilges, M., Pannu, N. S., Read, R. J., Rice, L. M., Simonson, T., and Warren, G. L. (1998) Crystallography & NMR system: A new software suite for macromolecular structure determination, *Acta Crystallogr. D54*, 905−921.
26. McCoy, A. J., Grosse-Kunstleve, R. W., Storoni, L. C., and Read, R. J. (2005) Likelihood-enhanced fast translation functions, *Acta Crystallogr. D61*, 458−464.
27. Lamzin, V. S., and Wilson, K. S. (1993) Automated refinement of protein models, *Acta Crystallogr. D49*, 129−147.
28. Lorimer, G. H., Badger, M. R., and Andrews, T. J. (1976) The activation of ribulose-1,5-bisphosphate carboxylase by carbon dioxide and magnesium ions. Equilibria, kinetics, a suggested mechanism, and physiological implications, *Biochemistry 15*, 529−536.
29. Andersson, I. (1996) Large structures at high resolution: The 1.6 Å crystal structure of spinach ribulose-1,5-bisphosphate carboxylase/oxygenase complexed with 2-carboxyarabinitol bisphosphate, *J. Mol. Biol. 259*, 160−174.

BI7000483